

## Research Article

# Optimal Control and Cost-Effectiveness Strategies of Malaria Transmission with Impact of Climate Variability

**Temesgen Duressa Keno** , **Lemesa Bedjisa Dano** , and **Gamachu Adugna Ganati** 

*Department of Mathematics, Wollega University, Nekemte, Ethiopia*

Correspondence should be addressed to Temesgen Duressa Keno; [temesgenduressaa@gmail.com](mailto:temesgenduressaa@gmail.com)

Received 26 April 2022; Revised 6 May 2022; Accepted 12 May 2022; Published 29 June 2022

Academic Editor: Kenan Yildirim

Copyright © 2022 Temesgen Duressa Keno et al. This is an open access article distributed under the Creative Commons Attribution License, which permits unrestricted use, distribution, and reproduction in any medium, provided the original work is properly cited.

We proposed in this study a deterministic mathematical model of malaria transmission with climate variation factor. In the first place, fundamental properties of the model, such as positivity of solution and boundedness of the biological feasibility of the model, were proved whenever all initial data of the states were nonnegative. The next-generation matrix method is used to compute a basic reproduction number with respect to the disease-free equilibrium point. The Jacobian matrix and the Lyapunov function are used to check the local and global stability of disease-free equilibria. If the basic reproduction number is less than one, the model's disease-free equilibrium points are both locally and globally asymptotically stable; otherwise, an endemic equilibrium occurs. The results of the sensitivity analysis of the basic reproduction numbers were obtained, and its biological interpretation was provided. The existence of bifurcation was discussed, and the model exhibits forward and backward bifurcations with respect to the first and second basic reproduction numbers, respectively. Secondly, using the maximum principle of Pontryagin, the optimal malaria reduction strategies are described with three control measures, namely, treated bed nets, infected human treatment, and indoor residual spraying. Finally, based on numerical simulations of the optimality system, the combination of treatment and indoor spraying is the most efficient and least expensive strategy for malaria eradication.

## 1. Introduction

Malaria is a serious vector-borne disease caused by a parasite called *Plasmodium* and transmitted between humans (hosts) and mosquitoes (vectors) through bites from infected female *Anopheles* mosquitoes [1]. It can spread through blood transfusions, needle sharing, or congenital causes. The parasites then reproduce in the human liver and bloodstream. Malaria is often associated with poverty, which has a negative impact on the country's economic development. According to the most recent global malaria report, published in December 2021, an estimated 241 million cases and 627000 deaths were reported worldwide, with the African region accounting for 94% of all cases in 2020 [2]. The use of insecticide-treated bed nets, antimalaria drug treatment, and indoor residual spraying are the most effective methods of preventing malaria transmission dynamics [3]. Most

mosquito distributions worldwide have been influenced by climatic factors such as temperature, rainfall, and malaria transmission increases with temperatures ranging from 16°C to 28°C, which create conducive conditions for mosquito breeding rates [4].

Ross [5] initiated a mathematical model on the dynamics of malaria spread. He developed SSSI models for human and malaria populations. According to Ross, reducing the number of mosquitoes to below a certain threshold is sufficient for malaria control. Following the Ross model, several models were proposed by scholars who extended the Ross model by considering various factors such as the exposure time in humans and mosquitoes [6–8] and climate variability on mosquito death rate, contact rate, and birth rate [9–11].

A group of researchers studied an optimal malaria transmission control model to determine the role of control measures in disease transmission. For example, Okosun et al.

[12] presented the malaria transmission dynamics with optimal control and cost-effectiveness analysis. The authors used a combination of three control measures: treated bed nets, antimalarial drug treatment of infected humans, and indoor residual spraying. They conclude that the combination of drug treatment of infected humans and indoor insecticide spraying is the most effective and least expensive way to prevent malaria spread. Makinde et al. [13] proposed a malaria model for disease spread with optimal control and cost-effectiveness analysis based on three control measures. Using the incremental cost-effectiveness ratio methods, a cost-effectiveness analysis was performed to support the results of the optimal control problem. The authors used numerical simulations to supplement the theoretical results. Finally, they proposed that a combination of treated bed nets, drug treatment, and indoor residual spraying is the most effective and less expensive intervention strategy. Okosun et al. [14] presented the SEIRS-SEI malaria transmission model with optimal control and cost-effectiveness analysis using combinations of three control measures, including treated bed nets, infected human treatment, and indoor residual spraying. The authors presented the use of infected human treatment with drugs and indoor residual spraying as the most cost-effective controls to prevent malaria spread. Otieno et al. [15] presented a malaria transmission model with an optimal control problem, employing four time-dependent control measures. Pontryagin's minimum principle was described in order to derive the necessary conditions for optimal malaria control. Their findings concluded that a combination of treated bed nets, treatment, and spraying is the most effective strategy for mitigating disease. Temesgen et al. [16] presented SIRS for the human population and SI malaria model for malaria transmission by incorporating three continuous controls. The authors suggested that combinations of treatment of infected humans and indoor residual spraying are the best strategies for the prevention of the disease.

However, none of these models take into account the impact of climate variability on malaria epidemics with optimal control and cost-effectiveness analysis with a logistic growth of climate variation with respect to mosquito breeding and malaria infection. In this paper, the malaria transmission model [17] is extended to the optimal control problem in the presence of climate variability in mosquito breeding rate and malaria infection, and further analysis on the least cost strategy is considered using the concept of cost-effectiveness analysis.

This paper is arranged as follows: In Section 2, we propose a malaria transmission model that shows the role of climate variability in malaria epidemics. In Section 3, the model analysis of the model is illustrated. In Section 4, we describe the analysis of sensitivity. In Section 5, the optimal control of the malaria transmission model is analytically analyzed using the maximum principle of Pontryagin. In Section 6, we show the simulation of theoretical results. In Section 7, the analysis of cost-effectiveness is depicted. The conclusion of the work is discussed in Section 8.

## 2. Model Description and Formulation

In this section, we developed a malaria transmission dynamics model in which the human population is represented by the SIRS model and the population of mosquitoes is described by the SI model due to their short lifespan. The total population of human at time  $(t)$  denoted by  $N_h(t)$  is divided into three subpopulations based on their disease status; susceptible humans  $S_h(t)$  are individuals who are vulnerable to risk of developing an infection from the mosquito. Infected humans  $I_h(t)$  are individuals who show the symptom of the disease and can transmit the disease to mosquito. Recovered humans  $R_h(t)$  are individuals who got temporary immunity, so that the total human populations is given by  $N_h(t) = S_h(t) + I_h(t) + R_h(t)$ . Individuals who are born or migrate are assumed to be susceptible human populations and considered as the recruitment rate denoted by  $\Psi$ . Susceptible human populations become infected if they come into contact with infected mosquitoes at the rate  $\beta_h(T, R)$  which depends on climate change,  $\beta_{0h}$  represents the human contact rate with vector when there is no climate variation, and  $\beta_{1h}$  denotes the human incremental contact rate due to climate variation. Humans leave the total population with a death rate  $\mu_h$ , and due to malaria disease, the induced death rate  $\delta$  reduces the population of human. Infected human recovered through treatment rate  $\gamma_h$  using antimalarial drugs. The recovered human population whose immunity is not permanent can lose it and become susceptible to reinfection at the rate  $\omega_h$ . The total vector population given by  $N_m(t)$  at time  $(t)$  is subgrouped into susceptible mosquito  $S_m(t)$  and infected mosquito  $I_m(t)$ . Hence, the total vector population is given by  $N_m(t) = S_m(t) + I_m(t)$ . The vector population is recruited at the rate  $\Phi(T, R)$  which depends on climate change, whereas  $\Phi_0$  denotes the vector birth rate when there is no climate variation and  $\Phi_{1m}$  is the vector incremental birth rate due to variation of climate. A mosquito population gets an infection when it contacts with infected human at the rate  $\beta_m(T, R)$  which depends on climate variation,  $\beta_{0m}$  represents the vector contact rate with a human when there is no climate change, and  $\beta_{1m}$  denotes incremental contact rate due to variations in climate. The vector natural death rate is  $\mu_m$ . We assume that mosquitoes do not recover from malaria disease. Thus, mosquitoes do not die due to disease infection. The growth rate of the temperature  $r$  follows a logistic function,  $m$  is the temperature-dependent rate of precipitation, and  $T_{\max}$  represents the maximum temperature for the mosquito to be most active, whereas the minimum temperature for the mosquito to be less active is denoted by  $T_0$ . Also, we have considered that the parameters stated in Table 1 are positive. Figure 1 illustrates the transmission dynamics of the malaria diagram.

Depending on the flowchart diagram in Figure 1, we write a model that governs the transmission dynamics of malaria disease using a system of ordinary differential equations.

$$\begin{cases} \frac{dS_h}{dt} = \Psi - \frac{\beta_h(T, R)}{1 + z * I_m} S_h I_m - \mu_h S_h + \omega_h R_h, \\ \frac{dI_h}{dt} = \Psi - \frac{\beta_h(T, R)}{1 + z * I_m} S_h I_m - (\mu_h S + \Upsilon_h) I_h, \\ \frac{dR}{dt} = \Upsilon_h I_h - (\mu_h + \omega_h) R_h, \\ \frac{dS_m}{dt} = \Phi(T) - \frac{\beta_m(T, R)}{1 + m * I_n} S_m I_h - \mu_m S_m, \\ \frac{dI_m}{dt} = r \left( 1 - \frac{T}{T_{\max}} \right) (T - T_0), \\ \frac{dR}{dt} = m \frac{dT}{dt} \Rightarrow R(t) = m(T(t) - T_0) + \varepsilon, \end{cases} \quad (1)$$

where

$$\begin{aligned} \beta_h(T, R) &= \beta_{0h} + \beta_{1h}k, \\ \beta_m(T, R) &= \beta_{0m} + \beta_{1m}k, \\ \Phi(T, R) &= \Phi_0 + \Phi_{1m}k, \\ k &= \frac{(1 + m)(T - T_0)}{T_{\max}}, \end{aligned} \quad (2)$$

with initial conditions

$$\begin{aligned} S_h(0) &= S_{h0}, \\ I_h(0) &= I_{h0}, \\ R_h(0) &= R_{h0}, \\ S_m(0) &= S_{m0}, \\ I_m(0) &= I_{m0}, \\ T(0) &= T_{m0}, \\ R(0) &= R_{m0}. \end{aligned} \quad (3)$$

Based on the fact that the average temperature at the Earth's surface rises, more evaporation occurs, which in turn increases overall precipitation (rainfall). Therefore, a warming climate is expected to increase precipitation (rainfall) in many areas. This implies that rainfall pattern is an increasing function of temperature. Note that  $m$  is the temperature-dependent rate of precipitation and  $\varepsilon$  is the amount of precipitation at  $T = T_0$ . In essence,

$$\begin{cases} R_0 = \varepsilon, & \text{when } T = T_0, \\ R_{\max} = m(T_{\max} - T_0) + R_0, & \text{when } T = T_m. \end{cases} \quad (4)$$

### 3. Mathematical Analysis of the Model

**3.1. Invariant Region.** The invariant region is used to determine where the model's solution is constrained. The proposed model (1) has two kinds of populations. Firstly, the total population of humans is given by

TABLE 1: Parameters' description used in system (1).

| Parameters   | Parameters' description                                 |
|--------------|---|
| $\Psi$       | The rate of new humans entering to population           |
| $\Phi_0$     | Mosquito population recruitment rate                    |
| $\gamma_h$   | Recover rate of the infected human                      |
| $\mu_h$      | Natural death rate of the human population              |
| $\delta$     | Human population induced death rate                     |
| $\mu_m$      | Mosquito natural death rate                             |
| $\omega_h$   | Immunity loss rate of human population                  |
| $\beta_{0h}$ | Human contact rate with population of mosquito          |
| $\Phi_{1m}$  | Increasing amount of vector breeding rate               |
| $\beta_{0m}$ | Contact rate of the mosquito with human                 |
| $z^*$        | Proportion of an antibody produced by human             |
| $\beta_{1m}$ | Increasing amount of vector contact rate                |
| $m^*$        | Proportion of an antibody produced by mosquito          |
| $\beta_{1h}$ | Increasing amount of human contact rate                 |
| $r$          | Growth rate of the temperature                          |
| $m$          | Temperature-dependent rate of precipitation             |
| $T_0$        | The smallest temperature that the vector is less active |
| $T_{\max}$   | Maximum temperature that the vector is the most active  |

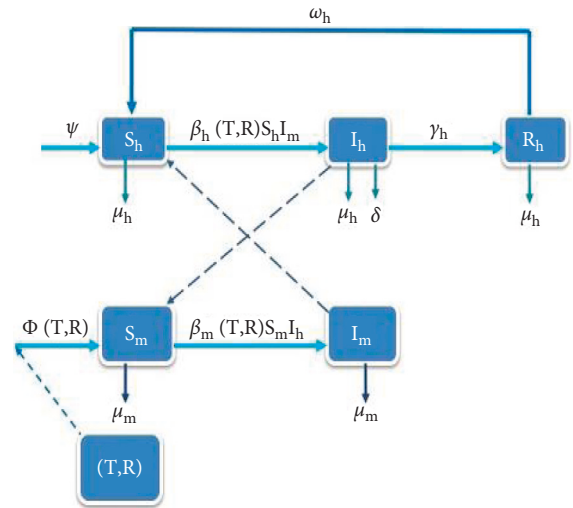


FIGURE 1: Transmission of malaria disease diagram.

$N_h(t) = S_h(t) + I_h(t) + R_h(t)$  and differentiating  $N_h(t)$  with respect to time. Then, by adding the first three equations from system (1), we obtain

$$\frac{d}{dt} (S_h + I_h + R_h) = \Psi - \mu_h N_h - \delta I_h. \quad (5)$$

This implies that equation (5) becomes

$$\frac{d}{dt} (S_h + I_h + R_h) \leq \Psi - \mu_h N_h. \quad (6)$$

By solving equation (6), we obtain that

$$0 < N_h \leq \frac{\Psi}{\mu_h}. \quad (7)$$

Thus, the invariant region of system (1) for the human population is a given by

$$\Omega_h = \left\{ (S_h, I_h, R_h) \in \mathbb{R}_+^3 : 0 < S_h + I_h + R_h \leq \frac{\Psi}{\mu_h} \right\}. \quad (8)$$

Secondly, the total number of the mosquito populations from system (1) is given as

$$N_m(t) = S_m(t) + I_m(t). \quad (9)$$

Hence, the differentiating  $N_m(t)$  with respect to time  $(t)$  is given by equation

$$\frac{d}{dt}(S_m + I_m) = \Phi(T, R) - \mu_m N_m. \quad (10)$$

By solving equation (10), we obtain  $0 < N_m \leq \Phi(T, R)/\mu_m$ . Hence, the invariant region of system (1) for the mosquito population is given by

$$\Omega_m = \left\{ (S_m, I_m) \in \mathbb{R}_+^2 : 0 < S_m + I_m \leq \frac{\Phi(T, R)}{\mu_m} \right\}. \quad (11)$$

Consequently, the dynamics of system (1) is studied in the biological feasible region of the form

$$\Omega = \Omega_h \times \Omega_m = \left\{ (S_h, I_h, R_h, S_m, I_m) \in \mathbb{R}_+^5 : N_h \leq \frac{\Psi}{\mu_h}, N_m \leq \frac{\Phi(T, R)}{\mu_m} \right\}, \quad (12)$$

which is a positive invariant set under the flow induced by the solution set of system (1).

**3.2. Positivity of the Solution.** For model (1), we will show that all solutions of system with positive initial data will remain positive for all times  $t \geq 0$ .

**Theorem 1.** *If  $S_h(0), I_h(0), R_h(0), S_m(0)$ , and  $I_m(0)$  are nonnegative, then the solutions  $S_h(t), I_h(t), R_h(t), S_m(t)$ , and  $I_m(t)$  of system (1) are nonnegative for  $t \geq 0$ .*

*Proof.* The first equation from system (1) is given by

$$\begin{aligned} \frac{dS_h}{dt} &= \Psi - \frac{\beta_h(T, R)S_h I_m}{1 + z^* I_m} - \mu_h N_h + \omega_h R_h, \\ \frac{dS_h}{dt} &\geq - \left( \frac{\beta_h(T, R)I_m}{1 + z^* I_m} + \mu_h \right) S_h. \end{aligned} \quad (13)$$

Integrating equation (13) with respect to time and using the method of separation variables with applying the initial conditions, we obtain

$$S_h(t) \geq S_h(0)e^{-((\beta_h(T, R)I_m / (1 + z^* I_m) + \mu_h)t)} \geq 0. \quad (14)$$

Clearly, equation (13) is nonnegative at all time  $t \geq 0$ . The other state variables  $I_h(t), R_h(t), S_m(t)$ , and  $I_m(t)$  are nonnegative for all time  $t \geq 0$  by the same procedure. As a result, the malaria transmission model stated in system (1) is both epidemiologically significant and mathematically well-posed in equation (12).  $\square$

**3.3. Basic Reproduction Numbers.** In the first place, we calculate the disease-free equilibrium (DFE) points of system (1) before calculating an expression for basic reproduction numbers. To do so, we equate all equations of model (1) to zero with  $I_h = 0$  and  $I_m = 0$ . In this case, we obtain two malaria-free equilibrium points of model (1), which are

given by  $E_1 = (S_h(0), I_h(0), R_h(0), S_m(0), I_m(0), T_0)$  or  $E_2 = (S_h(0), I_h(0), R_h(0), S_m(0), I_m(0), T_{\max})$  where

$$\begin{aligned} E_1 &= \left( \frac{\Psi}{\mu_h}, 0, 0, \frac{\Phi(T_0)}{\mu_m}, 0, T_0 \right), \\ \text{or } E_2 &= \left( \frac{\Psi}{\mu_h}, 0, 0, \frac{\Phi(T_{\max})}{\mu_m}, 0, T_{\max} \right). \end{aligned} \quad (15)$$

One advantage of determining the DFE of system (1) is to help us to calculate an expression for the basic reproduction number, which is defined as the average amount of secondary infections caused by a primary infectious in the given period [18]. It can be obtained using the approach of the next-generation matrix and that is the dominant eigenvalue of the next-generation matrix. For model (1), to obtain  $R_{01}$  and  $R_{02}$ , we rewrite model (1), beginning with newly infective classes of humans and mosquitoes, which are given by

$$\begin{aligned} \frac{dI_h}{dt} &= \frac{\beta_h(T, R)S_h I_m}{1 + z^* I_m} - (\mu_h + \delta + \gamma_h)I_h, \\ \frac{dI_m}{dt} &= \frac{\beta_m(T, R)S_m I_h}{1 + m^* I_h} - \mu_m I_m. \end{aligned} \quad (16)$$

The right-hand side (RHS) of equation (16) can be written in the form of  $f - v$ , where

$$\begin{aligned} f &= \begin{pmatrix} \frac{\beta_h(T, R)S_h I_m}{1 + z^* I_m} \\ \frac{\beta_m(T, R)S_m I_h}{1 + m^* I_h} \end{pmatrix}, \\ v &= \begin{pmatrix} (\mu_h + \delta + \gamma_h)I_h \\ \mu_m I_m \end{pmatrix}. \end{aligned} \quad (17)$$

The partial derivatives of  $f$  and  $v$  in equation (17) evaluated at DFE of system (1) produce two matrices  $F$  and  $V$ , respectively,

$$F = \begin{pmatrix} 0 & \beta_h(T, R) \frac{\Psi}{\mu_h} \\ \beta_m(T, R) \frac{\Phi(T, R)}{\mu_m} & 0 \end{pmatrix}, \quad (18)$$

$$V = \begin{pmatrix} \mu_h + \delta + \gamma_h & 0 \\ 0 & \mu_m \end{pmatrix}.$$

As a result, the basic reproduction number ( $R_0 = \rho(FV^{-1})$ ), where  $\rho$  is the dominant eigenvalue of  $FV^{-1}$ . Thus, the first basic reproduction number  $R_{01}$

calculated at the first disease-free equilibrium points  $E_1$  is given by

$$R_{01} = \sqrt{\frac{\beta_{0h} \Psi \beta_{0m} \Phi_0}{\mu_h \mu_m^2 (\mu_h + \delta + \gamma_h)}}. \quad (19)$$

Similarly, the second basic reproduction number  $R_{02}$  calculated at the second disease-free equilibrium points  $E_2$  is given by

$$R_{02} = \sqrt{\frac{(\beta_{0h} + \beta_{2h}) \Psi (\beta_{0m} + \beta_{2m}) (\Phi_0 + \Phi_{2m})}{\mu_h \mu_m^2 (\mu_h + \delta + \gamma_h)}}, \quad (20)$$

where  $\beta_{2h} = \beta_{1h}k, \beta_{2m} = \beta_{1m}k, \Phi_{2m} = \Phi_{1m}k$ , and  $k = (1 + m)(T_{\max} - T_0)/T_{\max}$ .

Generally, the basic reproduction number at maximum temperature ( $T_{\max}$ ) and rainfall variation in terms of  $R_{01}$  is given by

$$R_{02} = \sqrt{R_{01}^2 + \frac{\Phi_0 \beta_{0h} \beta_{2m} + \Psi (\beta_{0m} + \beta_{2m}) [\beta_{2h} (\Phi_0 + \Phi_{2m}) + \Phi_{2m} \beta_{0h}]}{\mu_h \mu_m^2 (\mu_h + \delta + \gamma_h)}}, \quad (21)$$

where  $R_{01}$  is the first basic reproduction number at  $(T_0, R_0)$  for the mosquito to be less active to breed.

### 3.4. Local Stability of Disease-Free Equilibrium

**Theorem 2.** *The disease-free equilibrium point of system (1) is locally asymptotically stable in  $\Omega$  if  $R_{01} < R_{02} < 1$ .*

*Proof.* We begin with finding that the Jacobian matrix of system (1) calculated at DFE is given by

$$J(E_*) = \begin{pmatrix} -\mu_h & 0 & \omega_h & 0 & -\beta_h(T^*, R^*) \frac{\Psi}{\mu_h} \\ 0 & -\mu_h + \delta + \gamma_h & 0 & 0 & \beta_h(T^*, R^*) \frac{\Psi}{\mu_h} \\ 0 & \gamma_h & -(\omega_h + \mu_h) & 0 & 0 \\ 0 & -\beta_m(T^*, R^*) \frac{\Phi(T^*, R^*)}{\mu_m} & 0 & -\mu_m & 0 \\ 0 & \beta_m(T^*, R^*) \frac{\Phi(T^*, R^*)}{\mu_m} & 0 & 0 & -\mu_m \end{pmatrix}. \quad (22)$$

From equation (22), we can obtain the characteristic equation of the following form:

$$(-\lambda - \mu_h)(-\lambda - \mu_m)(-\lambda - (\mu_h + \omega_h))(\lambda^2 + a_1\lambda + a_2) = 0, \quad (23)$$

where

$$a_1 = \mu_m + \mu_h + \delta + \gamma_h,$$

$$a_2 = \mu_m \gamma_h + \mu_m \delta + \mu_m \omega_h - \frac{\beta_h(T^*, R^*) \Psi \beta_m(T^*, R^*) \Phi(T^*, R^*)}{\mu_m \mu_h}. \quad (24)$$

Hence, from equation (23), we have

$$\begin{aligned} \lambda_1 &= -\mu_h < 0, \\ \lambda_2 &= -\mu_m < 0, \\ \lambda_3 &= -(\mu_h + \omega_h) < 0. \end{aligned} \quad (25)$$

Another equation from equation (23) will be a second-degree polynomial

$$\lambda^2 + a_1\lambda + a_2 = 0. \quad (26)$$

By using the Routh–Hurwitz criteria [19], equation (26) has a negative real root if  $a_1 > 0$  and  $a_2 > 0$ . Hence, we can observe that  $a_1 > 0$  since it is the sum of nonnegative

parameters and the value of  $a_2$  at  $(T^*, R^*) = (T_{\max}, R_{\max})$  is given by

$$a_2 = \mu_m \gamma_h + \mu_m \delta + \mu_m \mu_h - \frac{(\beta_{0h} + \beta_{2h})\Psi(\beta_{0m} + \beta_{2m})(\Phi_0 + \Phi_{2m})}{\mu_m \mu_h} = 1 - R_{02}^2 > 0. \tag{27}$$

It is worth noting from equation (27) that  $a_2 < 0$  if  $R_{02} < 1$ . Since  $R_{01} < R_{02}$ , so the DFE is locally asymptotically stable if  $R_{01} < R_{02} < 1$ .  $\square$

*Proof.* To discuss the global behavior of DFE of system (1), we use a technique implemented by the Lyapunov theorem [20] by first constructing a suitable Lyapunov function

$$V = \frac{\mu_m}{\beta_h(T^*, R^*)} I_h + I_m. \tag{28}$$

### 3.5. Global Stability of Disease-Free Equilibrium

**Theorem 3.** *If  $R_{01} < R_{02} < 1$ ,  $R_{01} < R_{02} < 1$ , then the disease-free equilibrium point(s) of system (1) is globally asymptotically stable in  $\Omega$ .*

By differentiating equation (28) with respect to time ( $t$ ), the result obtained becomes

$$\begin{aligned} \frac{dV}{dt} &= \frac{\mu_m}{\beta_h(T^*, R^*)} \frac{dI_h}{dt} + \frac{dI_m}{dt} \\ &= \frac{\mu_m}{\beta_h(T^*, R^*)} (\beta_h(T, R^*)S_h I_m - (\mu_h + \delta + \gamma_h)I_h) + \beta_m(T^*, R^*)S_m I_h - \mu_m I_m \\ &= \mu_m S_h I_m - \frac{\mu_m}{\beta_h(T^*, R^*)} (\mu_h + \delta + \gamma_h)I_h + \beta_m(T^*, R^*)S_m I_h - \mu_m I_m \\ &= \left( \beta_m(T^*, R^*)S_m - \frac{\mu_m}{\beta_h(T^*, R^*)} (\mu_h + \delta + \gamma_h) \right) I_h - \mu_m (1 - S_h)I_m \\ &\leq \left( \beta_m(T^*, R^*)S_m - \frac{\mu_m}{\beta_h(T^*, R^*)} (\mu_h + \delta + \gamma_h) \right) I_h \\ &= \left( \beta_m(T^*, R^*) \frac{\Phi(T^*, R^*)}{\mu_m} - \frac{\mu_m}{\beta_h(T^*, R^*)} (\mu_h + \delta + \gamma_h) \right) I_h \\ &= \frac{\mu_m (\mu_h + \delta + \gamma_h)}{(\beta_{0h} + \beta_{2h})} \left( \frac{\mu_h R_{02}^2}{\Psi} - 1 \right) I_h. \end{aligned} \tag{29}$$

Consequently, we observe that  $(dV/dt) < 0$  if  $R_{02} < 1$  and  $(dV/dt) = 0$  if and only if  $I_h = 0, I_m = 0$ . So, the dominant bounded invariant set  $\Gamma = \{(S_h, I_h, R_h, S_m, I_m) \in \Omega: (dV/dt) = 0\}$  is the singleton which is DFE in  $\Omega$ . Therefore, by the well-known LaSalle’s invariant principle [21], every solution that begins in the domain bounded invariant set approaches DFE as time tends to infinity when  $R_{01} < R_{02}$ . Therefore, the DFE is globally asymptotically stable in  $\Omega$  if  $R_{01} < R_{02} < 1$ .  $\square$

**3.6. Malaria Present Equilibrium.** Malaria endemic equilibrium point is a situation where malaria exists in the human population regardless of time and other factors. The endemic equilibrium point  $E^* = (S_h^*, I_h^*, R_h^*, S_m^*, I_m^*, T^*, R^*)$  can be obtained by setting RHS of all model equations of system (1) equal to zero. From model (1), the malaria present equilibrium point at  $(T^*, R^*) = (T_0, R_0)$  is given by

$$\begin{cases} S_h^* = \frac{(1 + z^* I_m)\psi + \omega_h R_h^*}{\beta_{0h} I_m^* + \mu_h (1 + z^* I_m)}, \\ R_h^* = \frac{\gamma_h I_h^*}{\omega_h + \mu_h}, \\ S_m^* = \frac{\Phi_0 (1 + m^* I_h)}{\beta_{0m} I_h^* + \mu_m (1 + m^* I_h)}, \\ I_m^* = \frac{\beta_{0m} S_h^* I_h^*}{\mu_m (1 + m^* I_h)}. \end{cases} \tag{30}$$

From equation (30), the endemic equilibrium easily satisfies the following polynomial and  $I_h^*$  is computed from the equation:

$$C_1 (I_h^*)^2 + C_2 (I_h^*) = 0, \tag{31} \quad \text{where}$$

$$\begin{aligned} C_1 &= \beta_{0m} (\beta_{0h} \Phi_0 (\omega_h \delta + \mu_h (\gamma_h + \omega_h + \delta + \mu_h)) + \mu_h (\omega_h + \mu_h) (\gamma_h + \delta + \mu_h) \mu_m), \\ C_2 &= (\omega_h + \mu_h) [\mu_h \mu_m^2 (\mu_h + \delta + \gamma_h) (1 - R_{01}^2)]. \end{aligned} \tag{32}$$

Hence,  $C_1 > 0$  and  $C_2 \geq 0$  whenever  $R_{01} \geq 1$ . Solving for  $I_h^*$  in equation (31), we obtain  $I_h^* = -(C_2/C_1) < 0$ . Thus, the model has no nonnegative malaria present equilibrium whenever  $R_{01} < 1$ . This guarantees that backward bifurcation does not exist in the model if  $R_{01} < 1$ .

Similarly, the endemic equilibrium point at  $(T^*, R^*) = (T_{\max}, R_{\max})$ , and solving for  $I_h^*$  as expression of parameters, we obtain

$$\begin{cases} S_h^* = \frac{(1 + z^* I_m) \psi + \omega_h R_h^*}{(\beta_{0h} + \beta_{2h}) I_m^* + \mu_h (1 + z^* I_m)}, \\ R_h^* = \frac{\gamma_h I_h^*}{\omega_h + \mu_h}, \\ S_m^* = \frac{\Phi_0 (1 + m^* I_h)}{(\beta_{0m} + \beta_{2m}) I_h^* + \mu_m (1 + m^* I_h)}, \\ I_m^* = \frac{(\beta_{0m} + \beta_{2m}) S_h^* I_h^*}{\mu_m (1 + m^* I_h)}, \end{cases} \tag{33}$$

where  $\beta_{2h} = \beta_{1k}, \beta_{2m} = \beta_{1k}, \Phi_{2m} = \Phi_{1k}$ , and  $k = (1 + m)(T - T_0)/T_{\max}$ .

From equation (33), the endemic equilibrium satisfies the following polynomial and  $I_h^*$  is computed from the equation

$$B_1 (I_h^*)^2 + B_2 (I_h^*) = 0, \tag{34}$$

where

$$\begin{aligned} B_1 &= \beta_{3m} (\beta_{3h} \Phi_{2m} (\omega_h \delta + \mu_h (\gamma_h + \omega_h + \delta + \mu_h)) + \mu_h (\omega_h + \mu_h) (\gamma_h + \delta + \mu_h) \mu_m), \\ B_2 &= (\omega_h + \mu_h) [\mu_h \mu_m^2 (\mu_h + \delta + \gamma_h) (1 - R_{02}^2)], \end{aligned} \tag{35}$$

where  $\beta_{3h} = \beta_{0h} + \beta_{2h}, \beta_{3m} = \beta_{0m} + \beta_{2m}$ , and  $\Phi_{3m} = \Phi_0 + \Phi_{2m}$ .

From equation (35), we see that if  $R_{02} < 1$ , then it immediately implies that  $R_{01} < 1$  and DFE exists for both  $R_{01}$  and  $R_{02}$ . However,  $R_{01} < 1$  does not immediately imply  $R_{02} < 1$  as the value of  $R_{02}$  will be larger than unity that shows that whereas  $R_{01}$  present DFE. Thus,  $R_{02}$  may become an endemic situation or exhibit backward bifurcation while  $R_{01}$  undergoes forward bifurcation only.

### 4. Sensitivity Analysis

Malaria control and eradication strategies should focus on key parameters that have a significant impact on the basic reproduction number. The purpose of carrying out the sensitivity analysis of the basic model parameter is to identify a parameter that affects the basic reproduction number. Essentially, the robustness of system predictions to parameter values can be expressed using the normalized

sensitivity index of the basic reproduction number to the given basic parameters because the values of those parameters can increase or decrease a basic reproduction number and vice versa. This method relies on our knowledge of the parameters that have a large influence on the basic reproduction number ( $R_{02}$ ) in order to design the best disease control strategies. We used the technique described in [13, 22, 23] to perform the sensitivity analysis.

*Definition 1.* (See [13, 22, 24, 25]): The forward sensitivity index of  $R_0$ , which is differentiable with respect to a given basic parameter  $D$ , is defined as

$$\tau_k^{R_0} = \frac{\partial R_0}{\partial D} \times \frac{k}{R_0}. \tag{36}$$

The sensitivity index of  $R_{01}$  of model (1) with respect to parameter  $\beta_{0h}$ , for instance, is obtained as

$$\tau_{\beta_{0h}}^{R_{01}} = \frac{\partial R_{01}}{\partial \beta_{0h}} \times \frac{\beta_{0h}}{R_{01}} = \frac{1}{2\sqrt{\beta_{0h}\Psi\beta_{0m}\Phi_0/\mu_h\mu_m^2(\mu_h + \delta + \gamma_h)}} \times \frac{\Psi\beta_{0m}\Phi_0}{\mu_h\mu_m^2(\mu_h + \delta + \gamma_h)} \times \frac{\beta_{0h}}{R_{01}} = \frac{1}{2} > 0. \tag{37}$$

Using the same approach with respect to the rest of the parameters,  $\tau_{\beta_{0m}}^{R_{01}}, \tau_{\Psi}^{R_{01}}, \tau_{\Phi_0}^{R_{01}}, \tau_{\mu_h}^{R_{01}}, \tau_{\mu_m}^{R_{01}}, \tau_{\delta}^{R_{01}}, \tau_{\gamma_h}^{R_{01}}$  are computed, and the sensitivity indices are presented in Table 2.

By the same procedure, the sensitivity index of  $R_{02}$  of the model (1) with respect to  $\Psi$  is given as

$$\begin{aligned} \Pi_{\Psi}^{R_{02}} &= \frac{\partial R_{02}}{\partial \Psi} \times \frac{\Psi}{R_{02}} \\ &= \frac{1}{2\sqrt{(\beta_{0h} + \beta_{2h})\Psi(\beta_{0m} + \beta_{2m})(\Phi_0 + \Phi_{2m})/\mu_h\mu_m^2(\mu_h + \delta + \gamma_h)}} \times \frac{(\beta_{0h} + \beta_{2h})(\beta_{0m} + \beta_{2m})(\Phi_0 + \Phi_{2m})}{\mu_h\mu_m^2(\mu_h + \delta + \gamma_h)} \times \frac{\Psi}{R_{02}} = \frac{1}{2} > 0. \end{aligned} \tag{38}$$

Similarly, with respect to other basic parameters,  $\Pi_{\beta_{0h}}^{R_{02}}, \Pi_{\beta_{0m}}^{R_{02}}, \Pi_{\Psi}^{R_{02}}, \Pi_{\Phi_0}^{R_{02}}, \Pi_{\beta_{1m}}^{R_{02}}, \Pi_{\Phi_{1m}}^{R_{02}}, \Pi_{\mu_h}^{R_{02}}, \Pi_{\mu_m}^{R_{02}}, \Pi_{\delta}^{R_{02}}, \Pi_{\gamma_h}^{R_{02}}$  are computed, and the sensitivity indices are described in Table 3.

strategy. After incorporating the controls into the malaria transmission model (1), the obtained state equations are as follows:

**4.1. Interpretation of the Sensitivity Indices.** We described sensitivity indices of basic reproduction number ( $R_{02}$ ) with respect to eight basic parameters in Table 2. The output showed that the parameters with a positive sensitivity index increased the value of  $R_{01}$  as their values increased, while the rest of the parameters remained constant. And if the values of the parameters with negative indices are increased while the values of the other parameters remain constant, the value of  $R_{01}$  decreases. Similarly, the sensitivity indices of  $R_{02}$  with respect to eleven basic parameters are shown in Table 3. The parameters with positive sensitivity indices have a high impact on malaria transmission in the community as their values increase. The basic parameters with negative sensitivity indices increase the malaria disease if their values decrease while the other parameters remain constant. For example,  $\Pi_{\Psi}^{R_{02}} = 0.5$  shows that decreasing (increasing) the rate of the human recruitment by 10% decreases (increases) the basic reproduction number  $R_{02}$  by 5%; similarly,  $\Pi_{\mu_m}^{R_{02}} = -1$  indicates that decreasing (increasing) the rate of the mosquito death by 10% increases (decreases) the basic reproduction number  $R_{02}$  by 10%.

$$\left\{ \begin{aligned} \frac{dS_h}{dt} &= \Psi(1 - u_1) - \frac{\beta_h(T, R)}{1 + z^*I_m} S_h I_m - \mu_h S_h + \omega_h R_h, \\ \frac{dI_h}{dt} &= (1 - u_1) \frac{\beta_h(T, R)}{1 + z^*I_m} S_h I_m - (\mu_h + \delta + \gamma_h + u_2) I_h, \\ \frac{dR}{dt} &= (\gamma_h + u_1) I_h - (\mu_h + \omega_h) R_h, \\ \frac{dS_m}{dt} &= \Phi(T) - (1 - u_1) \frac{\beta_m(T, R)}{1 + m^*I_n} S_m I_h - (\mu_m + u_3) S_m, \\ \frac{dI_m}{dt} &= (1 - u_1) \frac{\beta_m(T, R)}{1 + m^*I_n} S_m I_h - (\mu_m + u_3) I_m, \\ \frac{dT}{dt} &= r \left( 1 - \frac{T}{T_{\max}} \right) (T - T_0), \\ \frac{dR}{dt} &= m \frac{dT}{dt} \Rightarrow R(t) = m(T(t) - T_0) + \varepsilon, \end{aligned} \right. \tag{39}$$

**5. Extension of the Model into Optimal Control**

According to the necessity and severity of a disease, many intervention strategies are applied by public health officials to control the disease [25]. In this study, we extended the malaria transmission model (1) to an optimal control problem to determine control strategy decisions involving a mathematical model of biological situations [30]. Using this method, we hope to demonstrate the best malaria prevention

where  $\beta_h(T, R) = \beta_{0h} + \beta_{1h}k, \beta_m(T, R) = \beta_{0m} + \beta_{1m}k, \Phi(T, R) = \Phi_0 + \Phi_{1m}$ , and  $k = ((1 + m)(T - T_0)/T_{\max})$ .

The control functions represent that the use of a treated bed net to protect against mosquitoes is  $u_1(t)$ , the treatment of infected humans with antimalarial drugs is  $u_2(t)$ , and the use of indoor residual spraying to kill mosquitoes is  $u_3(t)$ . The objective functional that we developed for the optimal control model (39) is given as

$$J(u_1, u_2, u_3) = \min \int_0^{t_f} \left[ D_1 I_h + D_2 I_m + \frac{1}{2} (C_1 u_1^2 + C_2 u_2^2 + C_3 u_3^2) \right] dt, \tag{40}$$

TABLE 2: Sensitivity indices of parameter.

| Parameter    | Sensitivity index |
|--------------|-------------------|
| $\Psi$       | 0.5               |
| $\Phi_0$     | 0.5               |
| $\beta_{0h}$ | 0.5               |
| $\beta_{0m}$ | 0.5               |
| $\mu_m$      | 1                 |
| $\mu_h$      | -0.087541         |
| $\delta$     | -0.485158         |
| $\gamma_h$   | -0.024462         |

TABLE 3: Sensitivity indices of parameter.

| Parameter    | Sensitivity index |
|--------------|-------------------|
| $\Psi$       | 0.5               |
| $\Phi_0$     | 0.072438          |
| $\beta_{0h}$ | 0.281659          |
| $\beta_{0m}$ | 0.305714          |
| $\Phi_{1m}$  | 0.079169          |
| $\beta_{1h}$ | 0.218341          |
| $\beta_{1m}$ | 0.224286          |
| $\mu_m$      | -1                |
| $\mu_h$      | -0.092541         |
| $\delta$     | -0.475258         |
| $\gamma_h$   | -0.024461         |

where  $t_f$  denoted the terminal time,  $D_1$  and  $D_2$  are weight constants for the infected human and mosquito,

respectively, and  $C_1, C_2,$  and  $C_3$  are weight constants for each control, respectively. The expression  $(1/2)B_i u_i^2$  represents the cost function that corresponds to the controls  $u_i(t)$  and is quadratic in the other pieces of literature [18, 31–34, 36–38]. The goal of the objective functional (40) is to reduce the total number of infected humans  $I_h(t)$ , infected mosquitoes  $I_m(t)$ , and control costs  $u_i(t)$ . The primary goal is to compute a triple optimal control  $u_1^*, u_2^*$ , and  $u_3^*$  such that

$$J(u_1^*, u_2^*, u_3^*) = \min \{J\}(u_1, u_2, u_3): u_1, u_2, u_3 \in \mathcal{G}, \quad (41)$$

where  $\mathcal{G} = (u_1, u_2, u_3): u_i(t)$  such that  $u_1, u_2,$  and  $u_3$  are Lebesgue measurable on  $t \in [0, t_f]$  with  $0 \leq u_i(t) \leq 1$  is the control set. The obtained Hamiltonian (H) function of the optimal control problem that consists of equations (39) and (40) is represented as

$$H = \left[ A_1 I_h + A_2 I_m + \frac{1}{2} \sum_{i=1}^3 B_i u_i^2 \right] + \lambda_1 \frac{dS_h}{dt} + \lambda_2 \frac{dI_h}{dt} + \lambda_3 \frac{dR_h}{dt} + \lambda_4 \frac{dS_m}{dt} + \lambda_5 \frac{dI_m}{dt} + \lambda_6 \frac{dT}{dt} + \lambda_7 \frac{dR}{dt}. \quad (42)$$

From equation (42), the minimize Hamiltonian function with respect to  $u_1, u_2, u_3$  is given by

$$\begin{aligned}
 H = & \left[ A_1 I_h + A_2 I_m + \frac{1}{2} B_1 u_1^2 + B_2 u_2^2 + B_3 u_3^2 \right] \\
 & + \lambda_1 \left( \Psi - (1 - u_1) \frac{\beta_h(T, R)}{1 + z^* I_m} S_h I_m - \mu_h S_h + \omega_h R_h \right) \\
 & + \lambda_2 \left( (1 - u_1) \frac{\beta_h(T, R)}{1 + z^* I_m} S_h I_m - (\mu_h + \delta + \gamma_h + u_2) I_h \right) \\
 & + \lambda_3 \left( (\gamma_h + u_2) I_h - (\mu_h + \omega_h) R_h \right) \\
 & + \lambda_4 \left( \Phi(T, R) - (1 - u_1) \frac{\beta_m(T, R)}{1 + m^* I_h} S_m I_h - (\mu_m + u_3) S_m \right) \\
 & + \lambda_5 \left( (1 - u_1) \frac{\beta_m(T, R)}{1 + m^* I_h} S_m I_h - (\mu_m + u_3) I_m \right) \\
 & + \lambda_6 r \left( 1 - \frac{T}{T_{\max}} \right) (T - T_0) \\
 & + \lambda_7 m r \left( 1 - \frac{T}{T_{\max}} \right) (T - T_0),
 \end{aligned} \quad (43)$$

where  $\lambda_1, \lambda_2, \lambda_3, \lambda_4, \lambda_5, \lambda_6,$  and  $\lambda_7$  are adjoint variables. Next, to obtain the costate variables by using Pontryagin's

maximum principle [32], with the existence result of [35], the following theorem is stated.

**Theorem 4.** Given optimal controls  $u_1^*, u_2^*, u_3^*$  and a solution  $S_h^*, I_h^*, R_h^*, S_m^*, I_m^*, T^*, R^*$  of the corresponding state system that minimize  $J(u_1, u_2, u_3)$  over  $\mathfrak{D}$  subject to equation (39),

then adjoint variables  $\lambda_1, \lambda_2, \lambda_3, \lambda_4, \lambda_5,$  and  $\lambda_6$  hold the adjoint system

$$\left\{ \begin{aligned} \frac{d\lambda_1}{dt} &= \left( (1 - u_1) \frac{\beta_h(T, R)}{1 + z^* I_m} I_m (\lambda_2 - \lambda_1) \right) + \mu_h \lambda_1, \\ \frac{d\lambda_2}{dt} &= \left( (1 - u_1) \frac{\beta_h(T, R)}{1 + z^* I_m} S_m (\lambda_5 - \lambda_4) \right) + \lambda_2 (\mu_h + \delta + \gamma_h + u_2) - \lambda_3 (\gamma_h + u_2)^{-D_1}, \\ \frac{d\lambda_3}{dt} &= -\omega_h \lambda_1 + \lambda_3 (\mu_h + \omega_h), \\ \frac{d\lambda_4}{dt} &= - \left( (1 - u_1) \frac{\beta_m(T, R)}{1 + m^* I_h} I_h (\lambda_5 - \lambda_4) \right) + \lambda_4 (\mu_m + u_3), \\ \frac{d\lambda_5}{dt} &= - \left( (1 - u_1) \frac{\beta_m(T, R)}{1 + m^* I_h} S_h (\lambda_2 - \lambda_1) \right) + \lambda_4 (\mu_m + u_3) - D_2, \\ \frac{d\lambda_6}{dt} &= r\lambda_6 - r\lambda_6 \left( \frac{T_0}{T_{\max}} - \frac{T}{T_{\max}} \right), \\ \frac{d\lambda_7}{dt} &= mr\lambda_7 - rm\lambda_7 \left( \frac{T_0}{T_{\max}} - \frac{T}{T_{\max}} \right). \end{aligned} \right. \tag{44}$$

With transversality conditions,

$$\begin{aligned} \lambda_1(t_f) &= \lambda_2(t_f) = \lambda_3(t_f) = \lambda_4(t_f) = \lambda_5(t_f) \\ &= \lambda_6(t_f) = \lambda_6(t_f) = \lambda_6(t_f) = 0. \end{aligned} \tag{45}$$

Furthermore, the optimal controls  $u_1^*, u_2^*, u_3^*$  are represented by

$$\begin{aligned} u_1^* &= \max \left\{ 0, \min \left\{ 1, \frac{(\lambda_2 - \lambda_1) \left( \beta_h(T, R) / 1 + z^* I_m \right) S_h^* I_m^* + (\lambda_5 - \lambda_4) \left( \beta_m(T, R) / 1 + m^* I_h \right) S_m^* I_h^*}{C_1} \right\} \right\}, \\ u_2^* &= \max \left\{ 0, \min \left\{ 1, \frac{(\lambda_2 - \lambda_3) I_h^*}{C_2} \right\} \right\}, \\ u_3^* &= \max \left\{ 0, \min \left\{ 1, \frac{\lambda_4 S_m^* + \lambda_5 I_m^*}{C_3} \right\} \right\}. \end{aligned} \tag{46}$$

*Proof.* To obtain the form of the costate equations, we compute the derivative of the Hamiltonian function (H) equation (42) with respect to  $S_h, I_h, R_h, S_m, I_m,$  and  $T,$  respectively. Then, the adjoint or costate equation obtained is given by

$$\left\{ \begin{aligned} \frac{d\lambda_1}{dt} &= -\left( (1-u_1) \frac{\beta_h(T,R)}{1+z^* I_m} I_m (\lambda_2 - \lambda_1) \right) + \mu_h \lambda_1, \\ \frac{d\lambda_2}{dt} &= -\left( (1-u_1) \frac{\beta_h(T,R)}{1+z^* I_m} S_m (\lambda_5 - \lambda_4) \right) + \lambda_2 (\mu_h + \delta + \gamma_h + u_2) - \lambda_3 (\gamma_h + u_2) - D_1, \\ \frac{d\lambda_3}{dt} &= -\omega_h \lambda_1 + \lambda_3 (\mu_h + \omega_h), \\ \frac{d\lambda_4}{dt} &= -\left( (1-u_1) \frac{\beta_m(T,R)}{1+m^* I_h} I_h (\lambda_5 - \lambda_4) \right) + \lambda_4 (\mu_m + u_3), \\ \frac{d\lambda_5}{dt} &= -\left( (1-u_1) \frac{\beta_m(T,R)}{1+m^* I_h} S_h (\lambda_2 - \lambda_1) \right) + \lambda_4 (\mu_m + u_3) - D_2, \\ \frac{d\lambda_6}{dt} &= r\lambda_6 - r\lambda_6 \left( \frac{T_0}{T_{\max}} - \frac{T}{T_{\max}} \right), \\ \frac{d\lambda_7}{dt} &= mr\lambda_7 - rm\lambda_7 \left( \frac{T_0}{T_{\max}} - \frac{T}{T_{\max}} \right). \end{aligned} \right. \tag{47}$$

With transversality conditions,

$$\begin{aligned} \lambda_1(t_f) &= \lambda_2(t_f) = \lambda_3(t_f) = \lambda_4(t_f) \\ &= \lambda_5(t_f) = \lambda_6(t_f) = \lambda_7(t_f) = 0. \end{aligned} \tag{48}$$

To obtain the control value, we compute the partial derivative of Hamiltonian given by

$$\frac{\partial H}{\partial u_i} = 0 \text{ for } i = 1, 2, 3. \tag{49}$$

Obviously, after a partial derivative of Hamiltonian with respect to the controls, the result becomes

$$\begin{aligned} 0 &= \frac{\partial H}{\partial u_1} = (\lambda_2 - \lambda_1) \left( \beta_h(T,R) / 1 + z^* I_m \right) S_h^* I_m^* + (\lambda_5 - \lambda_4) \left( \beta_m(T,R) / 1 + m^* I_h \right) S_m^* I_h^* + u_1 C_1, \\ 0 &= \frac{\partial H}{\partial u_2} = \lambda_3 I_h^* - \lambda_2 I_h^* + u_2 C_2, \\ 0 &= \frac{\partial H}{\partial u_3} = -(\lambda_4 S_m^* + \lambda_5 I_m^*) + u_3 C_3. \end{aligned} \tag{50}$$

Moreover, solving for controls variables from equation (50), we obtain

$$\begin{aligned} u_1^* &= \frac{\lambda_2 - \lambda_1 \left( \beta_h(T,R) / 1 + z^* I_m \right) S_h^* I_m^* + (\lambda_5 - \lambda_4) \left( \beta_m(T,R) / 1 + m^* I_h \right) S_m^* I_h^*}{C_1}, \\ u_2^* &= \frac{(\lambda_2 - \lambda_3) I_h^*}{C_2}, \\ u_3^* &= \frac{\lambda_4 S_m^* + \lambda_5 I_m^*}{C_3}. \end{aligned} \tag{51}$$

Rearranging the solution of (51) with the boundary condition of each control, we got

$$\begin{aligned}
 u_1^* &= \max \left\{ 0, \min \left\{ 1, \frac{(\lambda_2 - \lambda_1) (\beta_h(T, R) / 1 + z^* I_m) S_h^* I_m^* + (\lambda_5 - \lambda_4) (\beta_m(T, R) / 1 + m^* I_h) S_m^* I_h^*}{C_1} \right\} \right\}, \\
 u_2^* &= \max \left\{ 0, \min \left\{ 1, \frac{(\lambda_2 - \lambda_3) I_h^*}{C_2} \right\} \right\}, \\
 u_3^* &= \max \left\{ 0, \min \left\{ 1, \frac{\lambda_4 S_m^* + \lambda_5 I_m^*}{C_3} \right\} \right\}.
 \end{aligned}
 \tag{52}$$

Next, we will see the simulation of the optimality system to identify an optimal strategy that is most optimal to minimize the spread of malaria transmission.  $\square$

### 6. Numerical Simulation

In this study, we solved the optimality system and used the forward-backward sweep to solve the state and adjoint systems in order to obtain the optimal strategy. We used the forward fourth-order Runge–Kutta to solve the state equations (39) due to the initial value of state variables. Similarly, the adjoint equations are solved using backward fourth-order Runge–Kutta due to the transversality condition (45) having the solution of state functions and the value of optimal controls. The controls are then updated using a convex combination of the previous controls and the value from the optimality conditions (46). This situation will continue until two consecutive iterations are close enough to each other [30]. The initial conditions that we used for numerical simulation of the optimality system are  $S_h(0) = 120$ ,  $I_h(0) = 20$ ,  $R_h(0) = 10$ ,  $S_m(0) = 300$ ,  $I_m(0) = 30$ ,  $T(0) = 16^\circ\text{C}$ , and  $R(0) = 11$  mm, as well as the parameter values from Table 4. We used the following weight constant values for the states and controls:  $D_1 = 60$ ,  $D_2 = 80$ ,  $C_1 = 40$ ,  $C_2 = 100$ , and  $C_3 = 60$ . We used the following four strategies with different combinations of two controls at a time and three controls at a time to determine the impact of each control on malaria reduction.

**6.1. Strategy A: Combination of Use of Treated Bed Nets ( $\mathbf{u}_1$ ) and Treatment of Infected Humans ( $\mathbf{u}_2$ ).** We optimized the objective function (39) using the treated bed net  $u_1$  and the treatment of infected humans with antimalarial drugs  $u_2$  when the value of the indoor residual spraying  $u_3$  was set to zero. Also, as shown in Figure 2(a), if there are controls, the number of infected humans  $I_h$  decreases and then tends to zero, whereas the number of infected humans increases if there are no controls. Similarly, in Figure 2(b), we can see that the infected mosquito  $I_m$  decreases as the control strategy is used, whereas the infected mosquito increases in the uncontrolled case. The control profiles shown in Figure 2(c) with this strategy suggest that controls on treated

bed net  $u_1$  kept maximum level (100%) until the end of the implementation while infected human treatment using antimalarial drugs  $u_2$  retained its maximum bound for 6 days then gradually tended to a minimum after the 82nd day.

**6.2. Strategy B: Combination of Use of Treated Bed Net ( $\mathbf{u}_1$ ) and Indoor Spraying ( $\mathbf{u}_3$ ).** This strategy combined the treated bed net as a control  $u_1$  and indoor residual spraying as a control  $u_3$  to reduce total infected populations and costs associated with the treatment of infected humans  $u_2$ . We can see in Figure 3(a) that the amount of infected human  $I_h$  with controls decreases and reaches its lowest point. In contrast, when there are no controls, the number of infected humans increases to a certain point. According to Figure 3(b), an infected mosquito  $I_m$  decreases in the control strategy and decreases. To its minimum point, an infected mosquito increases in the uncontrolled case. According to the control profiles depicted in Figure 3(c), control on treated bed net  $u_1$  is maintained at its maximum(100%) for 171 days, while indoor residual spraying  $u_3$  is maintained at its maximum for 8 days before dropping to its lowest value after the 120th day.

**6.3. Strategy C: Combination of Treatment of Infected Humans ( $\mathbf{u}_2$ ) and Indoor Spraying ( $\mathbf{u}_3$ ).** In this study, we used a combination treatment of infected humans as control  $u_2$  and indoor residual spraying as control  $u_3$  to reduce total infected populations and save money. Figure 4(a) shows that when using this control strategy, the number of infected humans  $I_h$  decreases to its lowest value and becomes smaller when controls are used. In Figure 4(b), the infected mosquito  $I_m$  decreases in the occurrence of control strategy and then drops to its minimum values, whereas in the uncontrolled case, an infected mosquito increase is observed. With this approach, the control profiles in Figure 4(c) conclude that controls on the treatment of infected human  $u_2$  maintain upper level (100 percent) for 9 days, while the insecticides spray  $u_3$  maintains maximum level for 7 days and then declines to lower bound at the end of the 80th day.

**6.4. Strategy D: Use of Treated Bed Net ( $\mathbf{u}_1$ ), Treatment ( $\mathbf{u}_2$ ), and Indoor Spraying ( $\mathbf{u}_3$ ).** We used a combination of three continuous controls on the treated bed net  $u_1$ ; treatment of

TABLE 4: Parameter description and taken values for model (1).

| Parameters   | Parameters' description                        | Values         | References |
|--------------|--|----------------|------------|
| $\gamma_h$   | Infected human recover rate                    | 0.0035         | [19]       |
| $\Psi$       | Human population recruitment rate              | 0.071          | [26]       |
| $\Phi_0$     | Mosquito population recruitment rate           | <b>0.041</b>   | [22]       |
| $\mu_m$      | Mosquito population natural death rate         | <b>0.05</b>    | [19]       |
| $\mu_h$      | Human population natural death rate            | <b>0.00004</b> | [13]       |
| $\delta$     | Human population induced death rate            | <b>0.068</b>   | [27]       |
| $\omega_h$   | Immunity loss rate of human population         | <b>0.09</b>    | [17]       |
| $\beta_{1m}$ | Increasing amount of vector breeding rate      | <b>0.07</b>    | [17]       |
| $\beta_{1h}$ | Increasing amount of human contact rate        | <b>0.05</b>    | [28]       |
| $\Phi_{1m}$  | Increasing amount of vector contact rate       | <b>0.09</b>    | [28]       |
| $\beta_{0h}$ | Contact rate human with mosquito               | <b>0.03</b>    | [17]       |
| $\beta_{0m}$ | Contact rate of mosquito with human            | <b>0.04</b>    | [13]       |
| $z^*$        | Proportion of an antibody produced by human    | 0.06           | Assumed    |
| $m^*$        | Proportion of an antibody produced by mosquito | 0.04           | Assumed    |
| $m$          | Temperature-dependent rate of precipitation    | <b>0.08</b>    | Assumed    |
| $r$          | Temperature growth rate                        | <b>0.007</b>   | [28]       |
| $T_0$        | Minimum values of temperature                  | 16°C           | [13]       |
| $T_{\max}$   | Maximum values of temperature                  | 28°C           | [29]       |

infected human  $u_2$ ; and indoor residual spraying  $u_3$  to reduce the objective function (39). By implementing those three control strategies, we discovered that, in Figure 5(a), the amount of infected human  $I_h$  decreases and decreases to a minimum level, whereas the amount of infected human increases to a certain point if no control is used. In Figure 5(b), the infected population of mosquitoes  $I_m$  is decreasing and minimized to its lower bound when a control strategy is used, whereas in the absence of a control strategy, an increase in infected mosquitoes is observed. Using this strategy, the control profile in Figure 5(c) depicted that controls on treated bed net  $u_1$  and treatment  $u_2$  were kept at 100% coverage for 5 and 8 days, respectively. Then, treated bed net  $u_1$  and treatment  $u_2$  tend to their lowest bound after 80 days, whereas indoor spraying  $u_3$  retains its highest values (100 percent) for 162 days before dropping to the lowest level on the 100th day.

Figure 6 shows the existence of bifurcation for malaria transmission model. Bifurcation occurs. This implies that, in equation (13), if  $R_{02} < 1$ , this automatically implies that  $R_{01} < 1$  and DFE exists for both  $R_{01}$  and  $R_{02}$ . However,  $R_{01} < 1$  do not automatically describe  $R_{02} < 1$ ,  $R_{02} < 1$ , because the value of  $R_{02}$  may be larger than unity that shows that DFE ( $E_2$ ) may depict backward bifurcation while DFE ( $E_1$ ) only depicts forward bifurcation.

### 7. Cost-Effectiveness Analysis

In this study, we must determine the most effective and least expensive method of reducing disease transmission. We employed the incremental cost-effectiveness ratio method to arrive at this strategy (ICER). Using this technique, we incrementally compare more than one competing intervention; for example, one intervention could be compared to a second, less effective alternative. This approach was defined as the ratio of the difference in averted costs between two strategies to the difference in the total

number of infections saved [23]. We calculated the total cost avoided and total infections saved from the numerical simulation of the optimal control problem, and the control strategy is ordered in increasing order based on the total infections saved, as shown in Table 5. The amount of total infection saved is calculated by subtracting the total number of humans infected with malaria using control from the total number of humans infected with malaria without control, while the cost averted of each strategy was obtained by using the cost function represented by  $(1/2)C_1u_1^2$ ,  $(1/2)C_2u_2^2$ , and  $(1/2)C_3u_3^2$  over the time [17, 28]. The amount of the total infection saved and the total cost of all strategies with their ICER is given in Table 6.

The value of the cost-effectiveness ratio (ICER) is computed from the total number of saved populations and total cost of averted for each strategy given in Table 5, which is used to compare the differences between the two strategies as obtained and given by

$$\begin{aligned}
 \text{ICER}(B) &= \frac{6421.36}{3794.79} = 1.693, \\
 \text{ICER}(C) &= \frac{1955.46 - 6420.36}{4094.55 - 3792.79} = -14.99, \\
 \text{ICER}(A) &= \frac{6476.61 - 1958.46}{4116.46 - 4092.55} = 188.96, \\
 \text{ICER}(D) &= \frac{6492.28 - 6476.61}{4118.48 - 4116.46} = 7.76.
 \end{aligned}
 \tag{53}$$

With the above results, the number of infections saved with ICER for four different strategies is shown in Table 6.

Table 6 compares the interventions B and C. ICER(C) is less than ICER(B) as shown in the table.

It implies that strategy B is costly and has a low likelihood of saving people. As a result, C saves more people than B. Then, from the competing strategies, we have removed

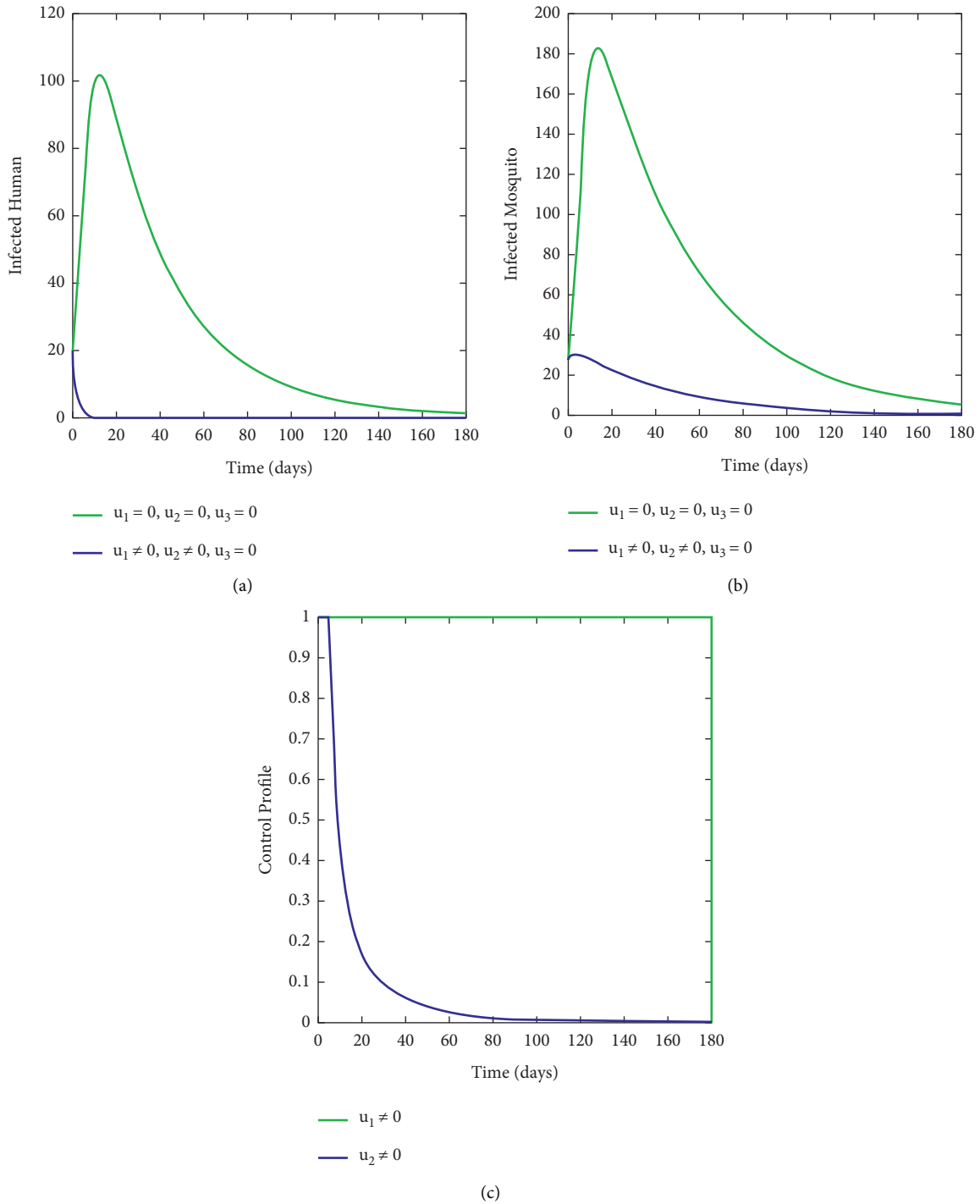


FIGURE 2: Simulation results showing the use of (a) treated bed net ( $u_1$ ), (b) treatment of infectious human ( $u_2$ ), and (c) the control profile for  $u_1, u_2 \neq 0$ .

B. Then, as shown in Table 7, calculate the ICER for the remaining strategies C, A, and D.

The ICER(A) is greater than the ICER(C) from the competing intervention strategies listed in Table 7. This demonstrates that ICER(C) strategy outperforms ICER(A). As a result, ICER(A) is less effective and more expensive than ICER(C). As a result, we removed strategy A from the

group of competing strategies and calculated the ICER as shown in Table 8.

Table 8 with intervention strategies C and D shows that ICER(C) is less than ICER(D). This indicates that strategy C strongly outperforms strategy D. As a result, the C strategy has the lowest total cost and is the most optimal. Based on the findings of the analysis, we believe that intervention C,

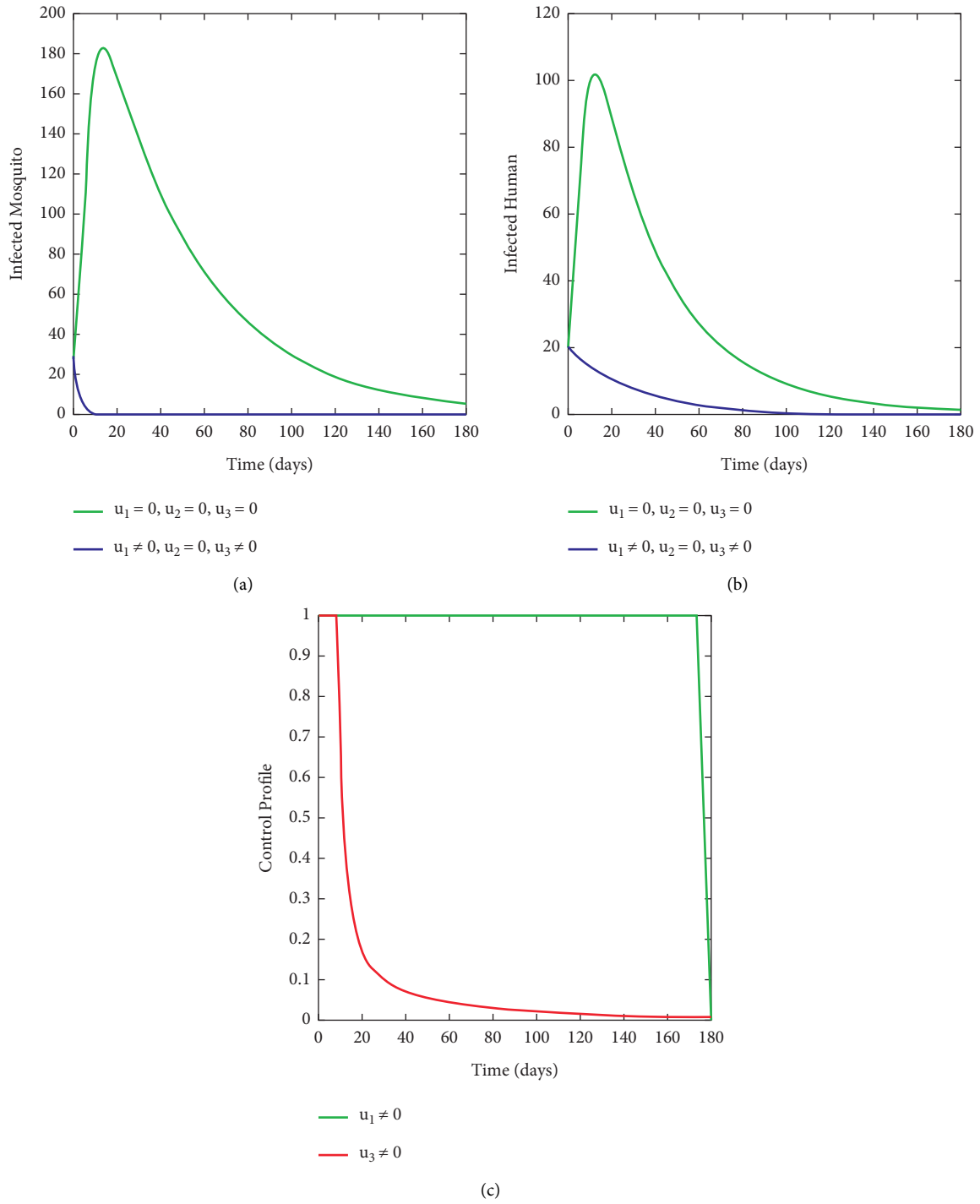


FIGURE 3: Simulation results depicting the use of (a) treatment of infectives ( $u_1$ ), (b) indoor spray of insecticides ( $u_3$ ), and (c) the control profile  $u_1, u_3 \neq 0$ .

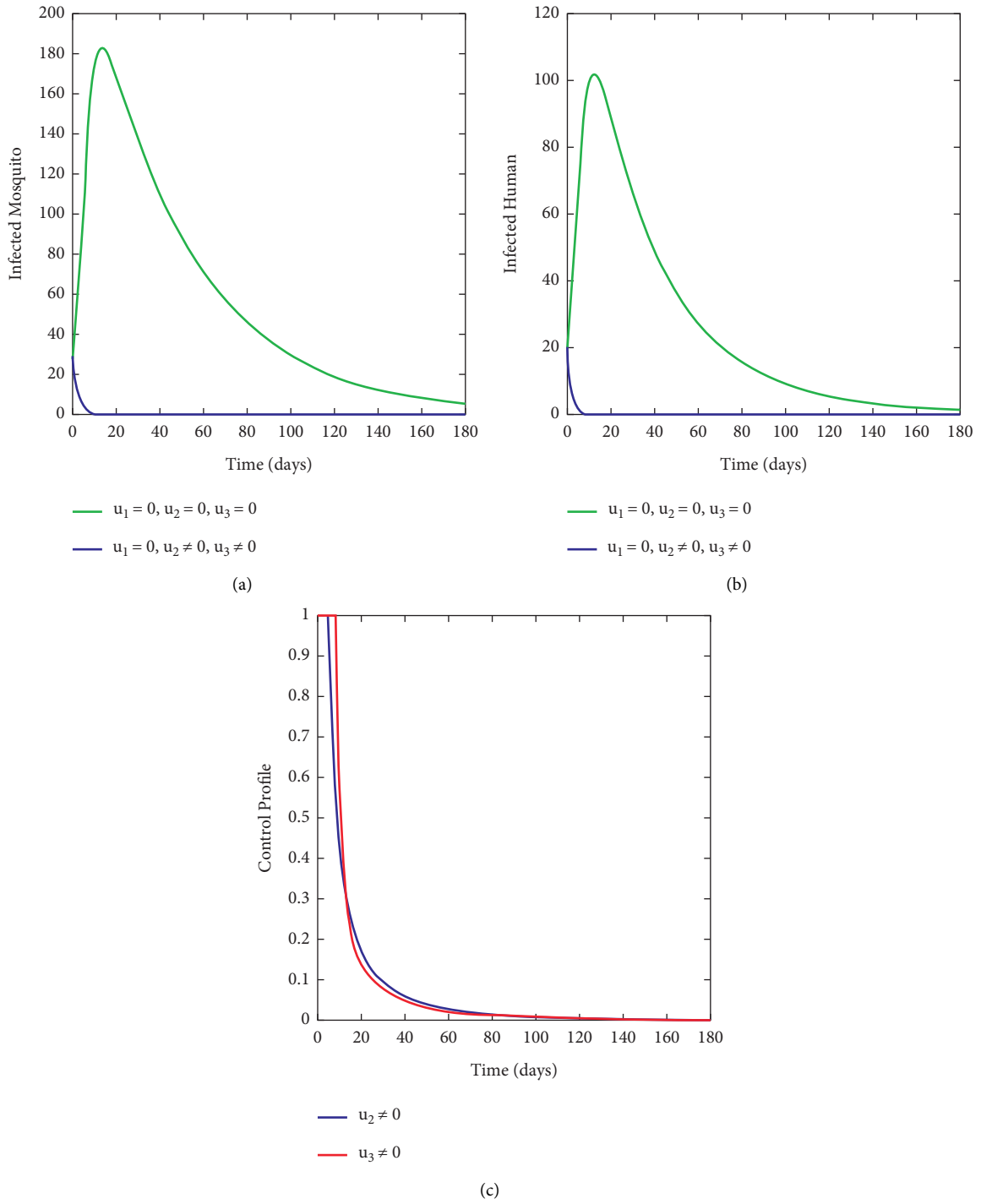


FIGURE 4: Simulation results representing (a) treatment of malaria infectious ( $u_2$ ), (b) indoor spray of insecticides ( $u_3$ ), and (c) the control profile for  $u_2, u_3 \neq 0$ .

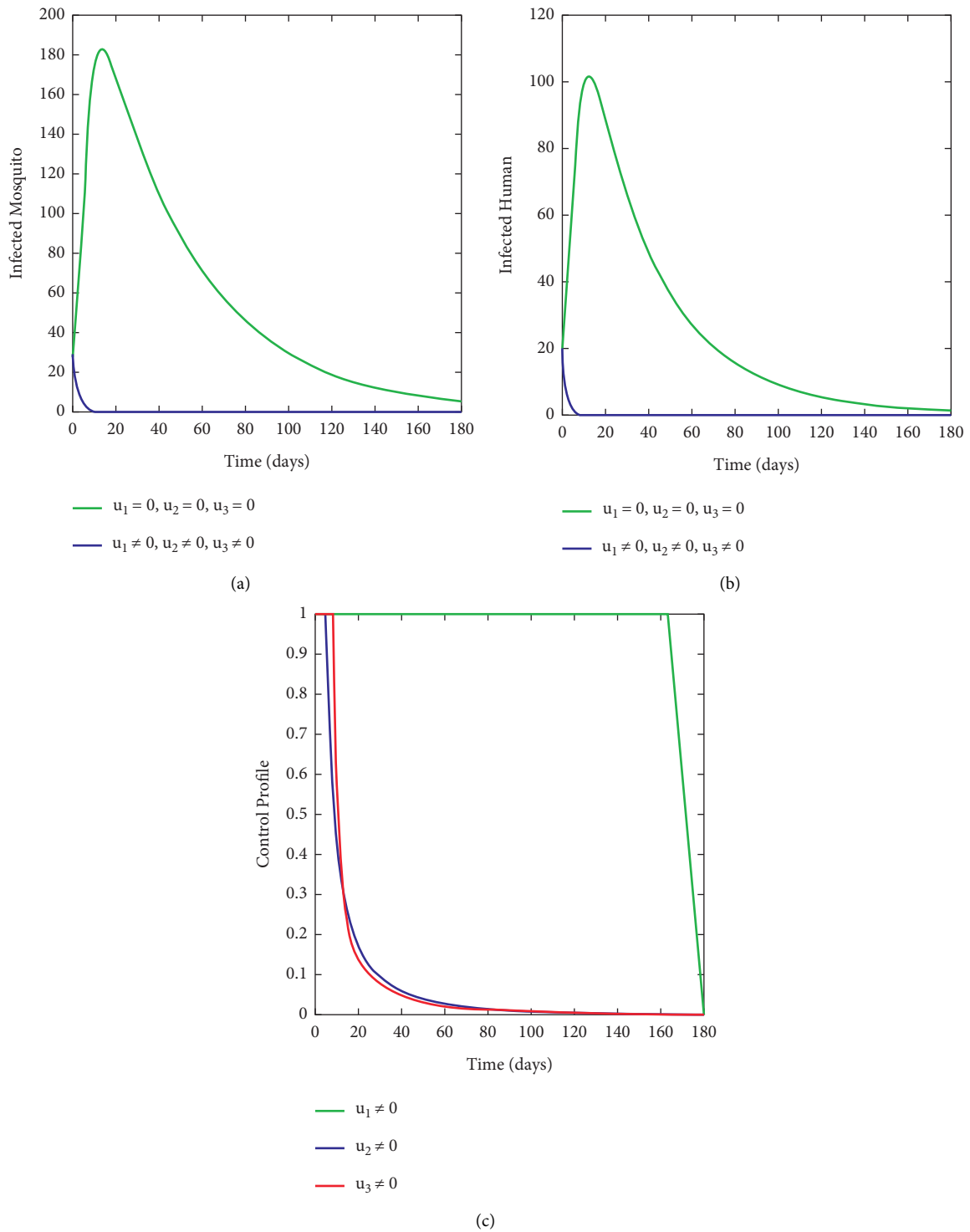


FIGURE 5: Simulation results indicating treated bed net ( $u_1$ ), treatment ( $u_2$ ), and insecticides spray ( $u_3$ ).

TABLE 5: Number of total infections saved and cost averted for all strategies.

| Strategy | Description                                  | Total infections averted | Total cost (\$) |
|----------|--|--------------------------|-----------------|
| A        | Treated bed net and insecticides spray       | 3794.79                  | 6421.36         |
| C        | Treatment of infected and insecticides spray | 4092.55                  | 1958.46         |
| B        | Treated bed net and treatment of infectious  | 4116.46                  | 6476.61         |
| D        | Treated bed net, treatment, and indoor spray | 4118.48                  | 6492.28         |

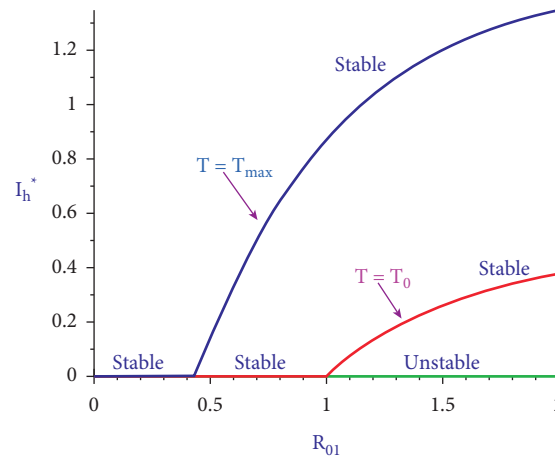


FIGURE 6: Diagram showing the existence of bifurcation when  $T = T_0$  and  $T = T_{max}$  for the malaria model problem.

TABLE 6: Amount of the total infection averted and total cost used with ICER.

| Strategy | Amount of infections saved | Total cost (\$) | ICER   |
|----------|----------------------------|-----------------|--------|
| B        | 3794.79                    | 6421.36         | 1.693  |
| C        | 4092.55                    | 1958.46         | -14.99 |
| A        | 4116.46                    | 6476.61         | 188.96 |
| D        | 4118.48                    | 6492.28         | 7.76   |

TABLE 7: Amount of the total infection averted and total cost used with ICER.

| Strategy | Amount of infections saved | Total cost (\$) | ICER   |
|----------|----------------------------|-----------------|--------|
| C        | 4092.55                    | 1958.46         | 2.09   |
| A        | 4116.46                    | 6476.61         | 188.96 |
| D        | 4118.48                    | 6492.28         | 7.76   |

TABLE 8: Amount of the total infection averted and total cost used with ICER.

| Strategy | Amount of infections saved | Total cost (\$) | ICER   |
|----------|----------------------------|-----------------|--------|
| C        | 4092.55                    | 1958.46         | 2.09   |
| D        | 4118.48                    | 6492.28         | 181.35 |

which consists of treating infected humans and spraying indoors, is the best optimal and least expensive strategy for limiting disease spread.

### 8. Conclusion

The impact of climate variability on malaria epidemics is described in this paper using deterministic mathematical modeling. The model analysis revealed qualitatively that the model's solution is both bounded and positive in the fixed domain. The method of the next-generation matrix is used to calculate the basic reproduction number with respect to the disease-free equilibrium. The Jacobian matrix and the

Lyapunov method are used to demonstrate the local stability and global stability of the disease-free equilibrium. Furthermore, if the basic reproduction number is less than one, the disease-free equilibrium is locally and globally asymptotically stable; otherwise, a positive endemic equilibrium occurs. The model's sensitivity has been described in detail, and the model demonstrates forward and backward bifurcation. According to the analytical findings, the best optimal way to prevent malaria epidemics is to reduce human-mosquito contact, increase mosquito death rates, and increase the treated rate of an infected human. Furthermore, we extended the model to an optimal control problem with three continuous controls, such as personal prevention with

a treated bed net, drug treatment of infected humans, and indoor residual spraying for mosquito minimizing strategy. The maximum principle of Pontryagin is applied to obtain the necessary conditions for optimal control, and the cost-effectiveness analysis is described for all combinations of the controls considered in the study. Based on the numerical analysis, we propose that the combination of treatment and indoor residual spraying is the best strategy for effectively reducing malaria.

## Data Availability

The data used to support the findings of this study are available from the corresponding author upon request.

## Conflicts of Interest

The authors have no particular conflicts of interest within the manuscript.

## References

- [1] J. Tumwiine, J. Y. T. Mugisha, and L. S. Luboobi, "A mathematical model for the dynamics of malaria in a human host and mosquito vector with temporary immunity," *Applied Mathematics and Computation*, vol. 189, no. 2, pp. 1953–1965, 2007.
- [2] World Health Organisation, *World Malaria Day, Report of the World Health Organisation*, (WHO), Geneva, Switzerland, 2021.
- [3] S. Olaniyi, K. O. Okosun, S. O. Adesanya, and R. S. Lebelo, "Modelling malaria dynamics with partial immunity and protected travellers: optimal control and cost-effectiveness analysis," *Journal of Biological Dynamics*, vol. 14, no. 1, pp. 90–115, 2020.
- [4] F. B. Augusto, A. B. Gumel, and P. E. Parham, "Qualitative assessment of the role of temperature variations on malaria transmission dynamics," *Journal of Biological Systems*, vol. 23, no. 04, pp. 1550030–1550630, 2015.
- [5] R. Ross, *The Prevention of Malaria*, John Murray, London, UK, 1911.
- [6] B. Traore, O. Koutou, and B. Sangare, "A global mathematical model of malaria transmission dynamics with structured mosquito population and temperature variations," *Nonlinear Analysis: Real World Applications*, vol. 53, Article ID 103081, 2020.
- [7] A. Nwankwo and D. Okuonghae, "Mathematical assessment of the impact of different microclimate conditions on malaria transmission dynamics," *Mathematical Biosciences and Engineering*, vol. 16, no. 3, pp. 1414–1444, 2019.
- [8] J. Mohammed-Awel, F. Augusto, R. E. Mickens, and A. B. Gumel, "Mathematical assessment of the role of vector insecticide resistance and feeding/resting behavior on malaria transmission dynamics: optimal control analysis," *Infectious Disease Modelling*, vol. 3, pp. 301–321, 2018.
- [9] G. J. Abiodun, P. Witbooi, and K. O. Okosun, "Mathematical Modelling and analysis of Mosquito-human malaria model," *Hacettepe Journal of Mathematics and Statistics*, vol. 47, pp. 219–235, 2018.
- [10] K. Okuneye, S. E. Eikenberry, and A. B. Gumel, "Weather-driven malaria transmission model with gonotrophic and sporogonic cycles," *Journal of Biological Dynamics*, vol. 13, pp. 288–324, 2019.
- [11] G. J. Abiodun, R. Maharaj, P. Witbooi, and K. O. Okosun, "Modelling the influence of temperature and rainfall on the population dynamics of *Anopheles arabiensis*," *Malaria Journal*, vol. 15, no. 1, pp. 364–381, 2016.
- [12] K. O. Okosun, R. Ouifki, and N. Marcus, "Optimal control analysis of a malaria transmission model that includes treatment and vaccination with waning immunity," *Bio-Systems*, vol. 106, pp. 136–145, 2011.
- [13] O. D. Makinde and K. O. Okosun, "Impact of chemo-therapy on optimal control of malaria disease with infected immigrants," *Biosystems*, vol. 104, no. 1, pp. 32–41, 2011.
- [14] K. O. Okosun, O. Rachid, and N. Marcus, "Optimal control strategies and cost-effectiveness analysis of a malaria model," *Biosystems*, vol. 111, no. 2, pp. 83–101, 2013.
- [15] G. Otieno, J. K. Koske, and J. M. Mutiso, "Transmission dynamics and optimal control of malaria in Kenya," *Discrete Dynamics in Nature and Society*, vol. 2016, Article ID 8013574, 27 pages, 2016.
- [16] D. K. Temesgen, O. D. Makinde, and L. L. Obsu, "Optimal control and cost effectiveness analysis of SIRS malaria disease model with temperature variability factor," *Journal of Mathematical and Fundamental Sciences*, vol. 53, no. 1, pp. 134–163, 2021.
- [17] D. K. Temesgen, O. D. Makinde, and O. L. Legesse, "Impact of Temperature Variability on SIRS Malaria model," *Journal of Biological Systems*, vol. 29, 2021.
- [18] P. Van den Driessche and J. Watmough, "Reproduction numbers and sub-threshold endemic equilibria for compartmental models of disease transmission," *Mathematical Biosciences*, vol. 180, no. 1–2, pp. 29–48, 2002.
- [19] M. Osman, I. Adu, and A. k. Isaac, "Simple mathematical model for malaria transmission," *Journal of Advances in Mathematics and Computer Science*, vol. 25, no. 6, pp. 1–24, 2017.
- [20] C. Castillo-Chavez, S. Blower, P. Driessche, D. Kirschner, and A. Yakubu, *Mathematical Approaches For Emerging And Reemerging Infectious Diseases: Models, Methods, And Theory*, Springer Science and Business Media, Berlin, Germany, 2002.
- [21] J. P. LaSalle, "The stability of dynamical systems, society for industrial and applied mathematics," in *Proceedings of the Conference Series in Applied Mathematics*, vol. 25, Cambridge, MA, USA, 1976.
- [22] N. Chitnis, J. M. Hyman, and J. M. Cushing, "Determining important parameters in the spread of malaria through the sensitivity analysis of a mathematical model," *Bulletin of Mathematical Biology*, vol. 70, no. 5, pp. 1272–1296, 2008.
- [23] S. Khajanchi, S. Bera, and T. K. Roy, "Mathematical analysis of the global dynamics of a HTLV-I infection model, considering the role of cytotoxic T-lymphocytes," *Mathematics and Computers in Simulation*, vol. 180, pp. 354–378, 2021.
- [24] L. B. Dano, K. P. Rao, and T. D. Keno, "Modeling the combined effect of hepatitis B infection and heavy alcohol consumption on the progression dynamics of liver cirrhosis," *Journal of Mathematics*, vol. 2022, Article ID 6936396, 18 pages, 2022.
- [25] D. K. Das, S. Khajanchi, and T. K. Kar, "The impact of the media awareness and optimal strategy on the prevalence of tuberculosis," *Applied Mathematics and Computation*, vol. 366, Article ID 124732, 2020.
- [26] A. M. Niger and A. B. Gumel, "Mathematical analysis of the role of repeated exposure on malaria transmission dynamics," *Differential Equations and Dynamical Systems*, vol. 16, no. 3, pp. 251–287, 2008.

- [27] M. A. Khan, A. Wahid, S. Islam, I. Khan, S. Shafie, and T. Gul, "Stability analysis of an SEIR epidemic model with non-linear saturated incidence and temporary immunity," *International Journal of Advances in Applied Mathematics and Mechanics*, vol. 2, pp. 1–14, 2015.
- [28] T. D. Keno, L. L. Obsu, and O. D. Makinde, "Modeling and optimal control analysis of malaria epidemic in the presence of temperature variability," *Asian-European Journal of Mathematics*, vol. 15, no. 01, p. 2250005, 2022.
- [29] G. Bhujju, G. R. Phaijoo, and D. B. Gurung, "Mathematical study on impact of temperature in malaria disease transmission dynamics," *Biomathematics*, vol. 1, no. 2, 2018.
- [30] S. Lenhart and J. T. Workman, *Optimal Control Applied to Biological Models*, Taylor and Francis, Abingdon-on-Thames, UK, 2007.
- [31] K. O. Okosun, M. Mukamuri, and D. O. Makinde, "Global stability analysis and control of leptospirosis," *Open Mathematics*, vol. 14, pp. 567–585, 2016.
- [32] L. S. Pontryagin, V. G. Boltyanskii, R. V. Gamkrelidze, and E. F. Mishchenko, *The Mathematical Theory of Optimal Processes*, Wiley, New York, NY, USA, 1962.
- [33] J. Mondal and S. Khajanchi, "Mathematical modeling and optimal intervention strategies of the COVID- outbreak," *Nonlinear Dynamics*, pp. 1–26, 2022.
- [34] S. Khajanchi, "Stability analysis of a mathematical model for glioma-immune interaction under optimal therapy," *International Journal of Nonlinear Sciences and Numerical Simulation*, vol. 20, no. 3-4, pp. 269–285, 2019.
- [35] W. H. Fleming and R. W. Rishel, *Deterministic and Stochastic Optimal Control*, Springer, Berlin, Germany, 1975.
- [36] K. O. Okosun, O. D. Makinde, and I. Takaidza, "Impact of optimal control on the treatment of HIV/AIDS and screening of unaware infectives," *Applied Mathematical Modelling*, vol. 37, no. 6, pp. 3802–3820, 2013.
- [37] K. R. Fister, S. Lenhart, and J. S. McNally, "Optimizing chemotherapy in an HIV model," *The Electronic Journal of Differential Equations*, vol. 32, pp. 1–12, 1998.
- [38] G. T. Tilahun, O. D. Makinde, and D. Malonza, "Modelling and Optimal Control of Typhoid Fever Disease with Cost-Effective Strategies," *Computational and Mathematical Methods in Medicine*, vol. 201716 pages, Article ID 2324518, 2017.